PNAS
www.pnas.org

Supplementary Information for

Complex dynamics under tension in a high-efficiency frameshift stimulatory structure

Matthew T.J. Halma, Dustin B. Ritchie, Tonia R. Cappellano, Krishna Neupane, Michael T. Woodside

Corresponding author: Michael Woodside
Email: michael.woodside@ualberta.ca

This PDF file includes:

www.pnas.org/cgi/doi/10.1073/pnas.1905258116

SUPPLEMENTARY METHODS

RNA constructs for SMFS: DNA encoding the 111-nt NS1′ frameshift signal of the WNV New York strain located downstream of the 7-nt slippery sequence and 5-nt spacer region (accession number NC_009942, nucleotides 3558 to 3668, sequence listed in Table S1) was inserted into the pMLuc1 plasmid between the SpeI and BamHI restriction sites to produce a transcription template. The frameshift signal was flanked in the transcription template on both sides by 3-nt linkers. This transcription template was first amplified by PCR, including 840-nt and 2240-nt segments of the plasmid respectively upstream and downstream of the frameshift signal for use as handles in SMFS, then the PCR product was transcribed *in vitro* with T7 RNA polymerase. Two single-stranded DNA handles, complementary 3′ and 5′ ends of the transcript and labeled respectively with biotin and digoxigenin, were produced by asymmetric PCR from double-stranded DNA PCR products corresponding to the flanking handle sequences (1). These handles were annealed with the RNA transcript, then the product was incubated with 600-nm and 820-nm diameter polystyrene beads labeled respectively with avidin DN (Vector Labs) and antidigoxigenin (Roche) to create dumbbells for optical trapping measurements. Dumbbells were diluted to ~2 pM in measuring buffer (50 mM MOPS, pH 7.0, 130 mM KCl, 4 mM $MgCl_2$), 50 U/mL Superase•In RNase inhibitor (Ambion), and oxygen-scavenging system (40 U/mL glucose oxidase, 185 U/mL catalase, and 8.3 mg/mL glucose) and inserted into a sample chamber on a clean microscope slide in the optical trap. For experiments including anti-sense oligomers, 10 μM of the DNA oligo (Integrated DNA Technologies) was added to the measurement buffer.

SMFS measurements and analysis: FECs were measured using a custom-built dual-trap optical tweezers setup. The stiffness of the two traps were 0.58 and 0.37 pN/nm, calibrated as described previously (2). The traps were moved apart with acousto-optic deflectors at a constant speed of 200 nm/s to unfold the RNA, while the position of the beads was measured with position-sensitive diodes sampled at 20 kHz and filtered online at 10 kHz using an 8-pole Bessel filter. After unfolding, the traps were brought together at the same speed to refold the RNA, and the RNA was held at ~ 0 pN for 3 s before the next unfolding curve was initiated. The speed of the force ramps resulted in a loading rate of ~20–80 pN/s in the force range of 5–13 pN; in comparison, the loading rate applied by a ribosome during translocation can be estimated from the ~80-ms translocation time (3) and the stiffness of the 5–6-nt linker between the slippery sequence and the stimulatory structure as ~100–400 pN/s in the same force range.

FECs were modeled as two extensible worm-like chains in series, one for the duplex handles and the other for the unfolded RNA. Each WLC was fit to the function

$$F(x) = \frac{k_B T}{L_p}\left[\frac{1}{4}\left(1 - \frac{x}{L_c} + \frac{F}{K}\right)^{-2} - \frac{1}{4} + \frac{x}{L_c} - \frac{F}{K}\right], \qquad (1)$$

where L_p is the persistence length, L_c the contour length, and K the elastic modulus (4). The same handle parameters (L_c, L_p, and K) were used in the fits for all branches of the FECs measured from a given molecule, and the RNA parameters L_p = 1 nm, K ~ 1500 pN (5) were taken as fixed constants in all fits, so that the only parameter varying between branches was the contour length of unfolded RNA, L_c^U. After fitting, each portion of the

FEC was assigned to a structural state based on the fits to determine the trajectory of states followed. The transition map was then generated by combining the state trajectories from all FECs.

Dual-luciferase frameshift assay: The sequence corresponding to *Renilla* luciferase and the multiple cloning site from pMLuc1 was cloned into the pISO plasmid (Addgene) upstream of the firefly luciferase sequence in pISO, with the firefly luciferase in the −1 frame, creating a dual-luciferase reporting system. Three variants were produced: (i) the desired WNV construct, with slippery sequence (C CCC UUU), linker region (CAG UU), and 111-nt stimulatory structure sequence (Table S1) inserted between the two luciferases using the PstI and SpeI restriction sites; (ii) a negative control with a stop codon replacing part of the slippery sequence, to measure the background level of frameshifting-independent firefly luciferase expression; and (iii) a positive control without a slippery sequence and with in-frame *Renilla* and firefly luciferase open reading frames, to measure the maximum expected firefly:*Renilla* luciferase ratio. For each construct, the transcription template was amplified by PCR and the transcribed *in vitro* with T7 RNA polymerase.

Frameshifting efficiency was measured by dual-luciferase assay (6). Briefly, 2 µg of mRNA from each construct was heated to 65 ^{o}C, mixed with 35 µL of treated rabbit reticulocyte lysate (Promega) and 0.5 µL of 1 mM amino-acid mixture lacking Leu and Met, and then incubated for 90 min at 30 ^{o}C. Using a microplate reader (Turner Biosystems) to measure luminescence from each of the constructs, 20 µL of each reaction was incubated with 100 µL of Dual-Glo Luciferase reagent (Promega) in a well for 10 min, before quantifying firefly luminescence. Then 100 µL of Dual-Glo Stop and Glo reagent was added to each well to quench firefly luminescence, and *Renilla* luminescence was measured after 10-min incubation. The −1 PRF efficiency was then calculated from the ratio of firefly and *Renilla* luminescence, subtracting the background measured from the negative control and normalizing by the positive control. Four replicates were measured and the results averaged.

SUPPLEMENTARY REFERENCES

1. K. Neupane, H. Yu, D. A. N. Foster, F. Wang, M. T. Woodside, Single-molecule force spectroscopy of the add adenine riboswitch relates folding to regulatory mechanism. *Nucleic Acids Res*. **39**, 7677–7687 (2011).
2. K. C. Neuman, S. M. Block, Optical trapping. *Rev. Sci. Instrum.* **75**, 2787–2809 (2004).
3. J.-D. Wen et al., Following translation by single ribosomes one codon at a time. *Nature* **452**, 598–603 (2008).
4. M. D. Wang, H. Yin, R. Landick, J. Gelles, S. M. Block, Stretching DNA with optical tweezers. *Biophys. J*. **72**, 1335–1346 (1997).
5. Y. Seol, G. M. Skinner, K. Visscher, Elastic properties of a single-stranded charged homopolymeric ribonucleotide. *Phys. Rev. Lett.* **93**, 8–11 (2004).
6. G. Grentzmann, J. A. Ingram, P. J. Kelly, R. F. Gesteland, J. F. Atkins, A dual-luciferase reporter system for studying recoding signals. *RNA* **4**, 479–486 (1998).

Table S1: RNA and DNA sequences. Sequences of the WNV frameshift signal and anti-sense DNA oligomers.

WNV frameshift signal	5′- GGG CCU UCU GGU CGU GUU CUU GGC CAC CCA GGA GGU CCU UCG CAA GAG GUG GAC AGC CAA GAU CAG CAU GCC AGC UAU ACU GAU UGC UCU GCU AGU CCU GGU GUU UGG GGG -3′
Oligo 1	5′-CUUGGCUGUCC-3′
Oligo 2	5′-CCCCCAAACACCAGG-3′

Table S2: Average contour length of unfolded RNA and refolding forces observed for each conformational state. Errors represent s.e.m.

State	L_c^U (nm)	F_R (pN)
DHP	0	7.5 ± 0.1
DHP−	10 ± 1	8.2 ± 0.1
PK_D	11 ± 2	6.8 ± 0.2
PK_D−	14 ± 2	7.7 ± 0.2
PK_A+HP	20 ± 1	8.5 ± 0.1
PK_A	31 ± 1	9.9 ± 0.3
$S1_A$	39 ± 1	11.1 ± 0.2

Table S3: Unfolding lengths and forces in presence of anti-sense oligos. State PK_D−* is a version of PK_D− in which stem 2 is shortened by 2 nt owing to strand invasion by oligo 2. Errors represent s.e.m.

With oligo 1				
Observed state	**Observed L_c^U (nm)**	**Proposed state**	**Expected L_c^U (nm)**	**Observed F_U (pN)**
1	0	DHP	0	10±1
2	12 ± 1	$S1_A$-4	11.8	16±1
3	19.5 ± 0.4	$S1_A$-3	18.1	15.5±0.2
4	29 ± 1	$S1_A$-2	29.9	18.5±0.3
5	41.8 ± 0.5	$S1_A$	40.9	16.3±0.3
U	61.3 ± 0.2	U	61.3	

With oligo 2				
Observed state	**Observed L_c^U (nm)**	**Proposed state**	**Expected L_c^U (nm)**	**Observed F_U (pN)**
1	14.2 ± 0.3	PK_D−*	13.7	19±2
2	21 ± 1	PK_A+HP	20.5	12±1
3	31 ± 1	PK_A	31.5	23±1
4	42 ± 1	$S1_A$	40.9	17±1
U	61.3 ± 0.3	U	47.6	

Table S4: State occupancies at the start of unfolding FECs and the end of refolding FECs. The occupancies observed at the start of unfolding, average over all curves, were similar to the occupancies observed for the first unfolding curve from each individual molecule. Error bars represent s.e.m.

State	Unfolding (all curves)	Unfolding (first pulls)	Refolding (all curves)
DHP	0.16 ± 0.02	0.13 ± 0.08	0.19 ± 0.02
DHP−	0.50 ± 0.02	0.50 ± 0.1	0.29 ± 0.02
PK_D	0.13 ± 0.02	0.13 ± 0.08	0.12 ± 0.02
PK_D−	0.08 ± 0.01	0.06 ± 0.06	0.08 ± 0.01
PK_A+HP	0.09 ± 0.01	0.13 ± 0.08	0.20 ± 0.02
PK_A	0.04 ± 0.01	0.06 ± 0.06	0.10 ± 0.01
$S1_A$	0	0	0.02 ± 0.01

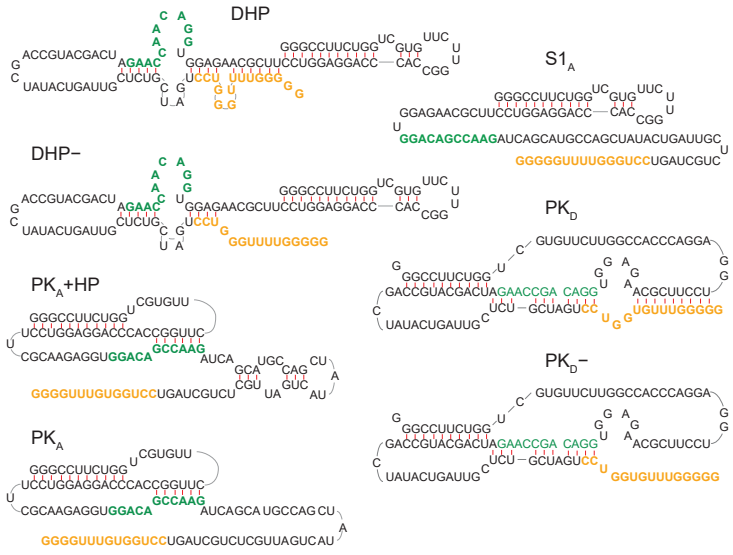

Figure S1: Secondary structure models of WNV frameshift signal conformations. Secondary structures are shown for each of the different conformations matching the states observed in the FECs, with base-pairing in red. The parts of the sequence complementary to anti-sense oligos 1 and 2 are indicated by green- and orange-colored bases, respectively.

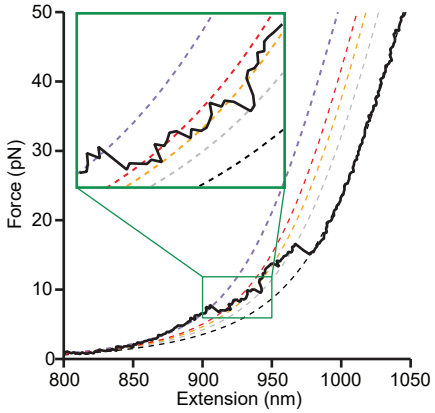

Figure S2: Reversible fluctuations between different conformations in FECs. Although FECs are inherently non-equilibrium measurements, some transitions were sufficiently close to equilibrium that reversible fluctuations between different structures could be observed. An example is shown here from an unfolding curve, with several examples of reversible 'hopping' between states highlighted in the inset. Dashed lines represent worm-like chain fits for DHP− (purple), PK_A+HP (red), PK_A (orange), $S1_A$ (grey), and unfolded (black).

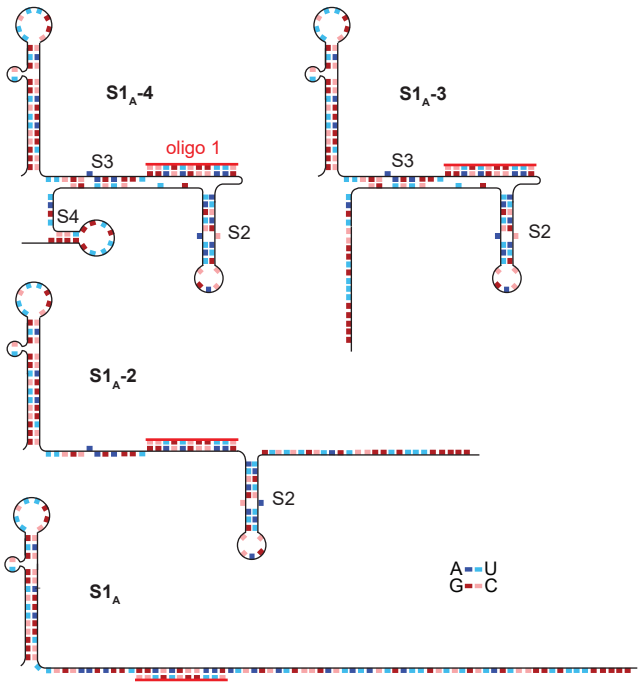

Figure S3: Secondary-structure models of states expected in the presence of oligo 1. One of the hairpins from the native folding ($S1_A$) remains, and three non-native helices (S2, S3, S4) can form.